Acta Cryst. (1996). B52, 976–981

Temperature Dependence of Crystal Structure of $NaK_{0.72}(NH_4)_{0.28}(+)$-$C_4H_4O_6.4H_2O$ in the Paraelectric Phase

EISUKE SUZUKI,* HITOSHI KABASAWA, TADAAKI HONMA, RYUSUKE NOZAKI AND YOICHI SHIOZAKI

Division of Physics, Graduated School of Science, Hokkaido University, Sapporo 060, Japan. E-mail: esuzuki@nirim.go.jp

(Received 26 July 1995; accepted 29 April 1996)

Abstract

The crystal structures of the ferroelectric $NaK_{0.72}(NH_4)_{0.28}(+)$-$C_4H_4O_6.4H_2O$ ($RS_{0.72}ARS_{0.28}$) have been studied in the paraelectric phase [$M_r = 276.32$, orthorhombic, $P2_12_12$, $Z = 4$, $F(000) = 575.04$, $\lambda(\text{Mo } K\alpha_1) = 0.70926$ Å]; $T =$ 213 (1), 253 (1) and 293 (1) K. The crystal data are as follows: (I) at $T = 213(1)$ K: $R = 0.0424$, $wR = 0.0399$, number of reflections = 3414, $a =$ 11.899 (2), $b = 14.273(2)$, $c = 6.211(1)$ Å, $V =$ 1054.9 (2) Å^3, $D_x = 1.740$ g cm^{-3}; (II) at $T =$ 253 (1) K: $R = 0.0498$, $wR = 0.0442$, number of reflections = 3284, $a = 11.929(1)$, $b = 14.297(1)$, $c =$ 6.221 (1) Å, $V = 1061.0(2)$ Å^3, $D_x = 1.730$ g cm^{-3}; (III) at $T = 293(1)$ K: $R = 0.0473$, $wR = 0.0392$, number of reflections = 3179, $a = 11.955(1)$, $b =$ 14.317 (1), $c = 6.231(1)$ Å, $V = 1066.5(1)$ Å^3, $D_x =$ 1.721 g cm^{-3}. X-ray investigations reveal details of structural change with temperature in the paraelectric phase. The carboxylate anion O(3)—C(4)—O(4) in the tartrate molecule is displaced along the a axis as the temperature decreases; moreover, the O(8) atom is displaced in the opposite direction against the shift of the carboxylate anion. The temperature dependence of the thermal motions of O(8) shows different behavior from the other oxygens of the water molecules. The amplitude of the thermal motion of O(8) does not tend to zero at $T = 0$ K, while the other oxygens of the water molecules tend to zero.

1. Introduction

Rochelle salt ($NaKC_4H_4O_6.4H_2O$, abbreviated here as RS) has a ferroelectric phase between the two transition temperatures of $T_{c1} = 297$ and $T_{c2} = 255$ K; the ferroelectric axis of RS is the a axis (Jona & Shirane, 1962). On the other hand, ammonium Rochelle salt ($NaNH_4C_4H_4O_6.4H_2O$, ARS) has one transition at $T_c = 109$ K, below which is polar along the b axis. The reversal of the spontaneous polarization of ARS cannot be achieved by the application of even a very strong electric field, but is easily realized by the application of the mechanical sheer stress (Takagi & Makita, 1958).

RS and ARS are isomorphous (orthorhombic, $P2_12_12$, $Z = 4$) in the paraelectric phase and they form a continuous series of mixed crystals over the whole range of concentration. The dielectric and pyroelectric properties of the mixed crystals have been investigated by Makita & Takagi (1958). The mixed-crystal system $NaK_{1-x}(NH_4)_xC_4H_4O_6.4H_2O$ (abbreviated as $RS_{1-x}ARS_x$) is divided into four compositional ranges (I–IV) according to the types of phase transition behavior.

The stable region of the ferroelectric phase of $RS_{1-x}ARS_x$ ($x = 0.0$–0.025) becomes narrower as the content x of ARS increases. Then it completely disappears at $x = 0.025$. This range is denoted as region I. In the compositional range from $x = 0.025$ to 0.18 a broad dielectric peak is observed, although no phase transition occurs (region II). In the range from $x = 0.18$ to 0.9 one dielectric peak is observed and another ferroelectric phase (the spontaneous polarization P_s is along the a axis) appears in a low-temperature region (region III). In the range from $x = 0.9$ to 1.0 the temperature dependence of the dielectric constant does not follow the Curie–Weiss law above the transition temperature and shows a small step at the transition temperature (region IV). The behavior of the polar phase in region IV is very similar to that of the low-temperature phase of ARS and the polarization is along the b axis.

The structural studies of RS in the ferroelectric phase (Suzuki & Shiozaki, 1996), which belongs in region I, have clarified that the O(8) atom in the water molecule and the carboxylate anion O(3)—C(4)—O(4) make a collective displacement in the ferroelectric phase (hereafter the numbers assigned to the atoms except for H atoms are as used by Beevers & Hughes, 1941).

The structural studies of $RS_{1-x}ARS_x$ mixed crystals ($x = 0.90$–1.00) at room temperature (Suzuki, Muta, Nozaki & Shiozaki, 1996), which belong in region IV, have clarified the dependence of the structural change on the content of ARS. The structural change due to the phase transition of ARS has been studied by Brózek & Stadnicka (1994) and Brózek, Mucha & Stadnicka

(1994). They reported that the structural change of the ferroelectric phase transition of ARS seems to rely on a cooperative process of the reorientation of NH_4^+ and water dipoles and also on the reorganization of the complex hydrogen-bonding network.

As mentioned above, P_s occurs along the a axis in regions I and III; however, the physical properties in both regions are different. Gesi & Ozawa (1980) have reported the dependence of the transition temperature on the hydrostatic pressure in $RS_{1-x}ARS_x$ mixed crystals. In region I both the upper and lower transition temperatures increase with increasing hydrostatic pressure, in region III the transition temperature decreases. El Saffar & Pope (1976) reported the effect of deuterium substitution on the transition temperature of this system. In region I the effect of deuteration is conspicuous and the stable region of the ferroelectric phase becomes wide. On the other hand, the transition temperature is practically unaffected by deuteration in region III, especially in the composition range $0.2 < x < 0.7$. These facts show the mechanisms of the phase transition in regions I and III are different.

It is also considered necessary for understanding the mixed-crystal system to study structural changes in region III and to compare the structures in regions I and III. The purpose of the present study is to determine the temperature dependence of the accurate crystal structure in the paraelectric phase in region III. In the present studies the mixed crystal $RS_{0.72}ARS_{0.28}$ has been investigated in the paraelectric phase ($T = 213$, 253 and 293 K).

2. Experimental

A single crystal of $NaK_{0.72}(NH_4)_{0.28}$(+)-$C_4H_4O_6.4H_2O$ was grown by slow evaporation of aqueous saturated solutions, $RS_{0.80}ARS_{0.20}$, of the following three salts: $2K_2$(+)-$C_4H_4O_6.H_2O$, Na_2(+)-$C_4H_4O_6.2H_2O$ and $(NH_4)_2$(+)-$C_4H_4O_6$. In the case of the preparation of the crystal, recrystallization was not carried out, because the content of ARS in the mixed crystal is different from that in aqueous solution.

The dielectric measurement was employed to determine the transition temperature and the content of ARS of the used sample. The content was estimated from the transition temperature using the phase diagram of Makita & Takagi (1958). As a result the transition temperature is 206 K and the content is ~ 0.28.

The sample crystal was sealed in a glass capillary tube to avoid dehydration and deliquescence. An automatic four-circle X-ray diffractometer (Rigaku AFC-5) was used with Mo $K\alpha_1$ radiation ($\lambda = 0.70926$ Å) monochromated by pyrolitic graphite. A cold nitrogen-gas-flow system was used in the measurement at $T = 213$ and 253 K. The observed intensities were corrected for Lorentz–polarization, absorption and extinction factors. The absorption correction (numerical integration) was made with the program *DABEX* (Dwiggins, 1975) in the *CHARGE* system. Lattice parameters are calculated with the following function for systematic errors of the lattice spacings: $\Delta d/d = \sin^2\theta\,(1/\sin\theta + 1/\theta)$. A summary of crystal data, data collections and refinements is listed in Table 1.

The $RS_{1-x}ARS_x$ mixed crystal has two nonequivalent special positions, (2*a*) and (2*b*) by Wyckoff notation. The two positions are occupied by the cations K^+ and NH_4^+. We will term the former position site (1) and the latter site (2). It is natural to consider that, in the mixed crystal, the accommodations of NH_4^+ for the two sites are different from each other. In order to specify the accommodation rates in the two sites, the two parameters α and β are introduced; α indicates the fraction of NH_4^+ accommodated in site (1) and β that in site (2). These parameters fulfill the relation $\alpha + \beta = 2x$.

As the initial values for the positional and thermal parameters of the refinements of the data at $T = 293$ K, the values for the crystal ($x = 1.00$) in region IV determined by Suzuki, Muta, Nozaki & Shiozaki (1996) were used. For the accommodation parameters α and β of NH_4^+ in the two sites, the contents of ARS obtained as the result of the dielectric measurement were used for the initial parameters ($\alpha = \beta = 0.28$). The final parameters of the crystal structure at $T = 293$ K were used as the initial values of the refinements at $T = 253$ and 213 K. Isotropic secondary extinction corrections and also full-matrix least-squares calculations were made with the program *RADIEL* (Coppens *et al.*, 1979). Full-matrix least-squares calculations have been performed by minimizing the function $\Sigma w(|F_o| - |F_c|)^2$ with $w^{-1} = \sigma^2(F_o) + (aF_o)^2$.

The atomic- and anomalous-scattering factors were taken from *International Tables for X-ray Crystallography* (1974, Vol. IV). Two types of atomic-scattering factor for the H atoms were used. The spherical-bonded H-atom scattering factor (Stewart, Davidson & Simpson, 1965) was used for H atoms bonded to C atoms and the free H-atom scattering factor (*International Tables for X-ray Crystallography*, 1974, Vol. IV) was used for H atoms bonded to O and N atoms.

The accommodation parameters α and β were determined by least-squares calculations together with all the other structural parameters, including those of H atoms. In the least-squares calculations the atomic-scattering factor $f_{KN(1)}$ of a hypothetical atom KN at site (1), defined as $f_{KN(1)} = (1-\alpha)f_K + \alpha f_N$, was used, where f_K and f_N indicate the atomic-scattering factors of the K and N atoms, respectively. The atomic-scattering factor at site (2), defined as $f_{KN(2)} = (1-\beta)f_K + \beta f_N$, was used in a similar manner. The following constraints were applied in the calculations of parameters α and β: z(K atom) = z(N atom), U_{ij} (K atom) = U_{ij} (N atom) ($i, j = 1$–3). For the atomic positions and thermal parameters of the H atoms in NH_4^+, the values of ARS

Table 1. *Experimental details*

	213 K	253 K	293 K
Crystal data			
Chemical formula	$NaK_{0.72}(NH_4)_{0.28}(C_4H_4O_6).4H_2O$	$NaK_{0.72}(NH_4)_{0.28}(C_4H_4O_6).4H_2O$	$NaK_{0.72}(NH_4)_{0.28}(C_4H_4O_6).4H_2O$
Chemical formula weight	276.32	276.32	276.32
Cell setting	Orthorhombic	Orthorhombic	Orthorhombic
Space group	$P2_12_12$	$P2_12_12$	$P2_12_12$
a (Å)	11.899 (2)	11.929 (1)	11.955 (1)
b (Å)	14.273 (2)	14.297 (1)	14.317 (1)
c (Å)	6.211 (1)	6.221 (1)	6.231 (1)
V (Å^3)	1054.9 (2)	1061.0 (2)	1066.5 (1)
Z	4	4	4
D_x (Mg m^{-3})	1.740	1.730	1.721
Radiation type	Mo $K\alpha_1$	Mo $K\alpha_1$	Mo $K\alpha_1$
Wavelength (Å)	0.70926	0.70926	0.70926
No. of reflections for cell parameters	30	30	30
θ range (°)	20–27.5	20–27.5	19.5–27.5
μ (mm^{-1})	0.4633	0.4606	0.4582
Temperature (K)	213	253	293
Crystal form	Sphere	Sphere	Sphere
Crystal diameter (mm)	0.50	0.50	0.50
Crystal color	Colorless	Colorless	Colorless
Data collection			
Diffractometer	Rigaku AFC-5	Rigaku AFC-5	Rigaku AFC-5
Data collection method	ω (2θ < 30°), 2θ–ω (30° < 2θ) scans	ω (2θ < 30°), 2θ–ω (30° < 2θ) scans	ω (2θ < 30°), 2θ–ω (30° < 2θ) scans
Absorption correction	Numerical integration (*DABEX*; Dwiggins, 1975)	Numerical integration (*DABEX*; Dwiggins, 1975)	Numerical integration (*DABEX*; Dwiggins, 1975)
T_{min}	0.8414	0.8423	0.8436
T_{max}	0.8423	0.8436	0.8451
No. of measured reflections	3982	4160	4195
No. of independent reflections	2000	1989	1937
No. of observed reflections	3414	3284	3179
Criterion for observed reflections	$F_o > 3\sigma(F_o)$	$F_o > 3\sigma(F_o)$	$F_o > 3\sigma(F_o)$
R_{int}	0.0257	0.0344	0.0245
θ_{max} (°)	35	37.5	40
Range of h, k, l	$0 \rightarrow h \rightarrow 19$ $0 \rightarrow k \rightarrow 23$ $-10 \rightarrow l \rightarrow 10$	$0 \rightarrow h \rightarrow 20$ $0 \rightarrow k \rightarrow 24$ $-10 \rightarrow l \rightarrow 10$	$0 \rightarrow h \rightarrow 19$ $0 \rightarrow k \rightarrow 25$ $-11 \rightarrow l \rightarrow 11$
No. of standard reflections	3	3	3
Frequency of standard reflections	Every 100 reflections	Every 100 reflections	Every 100 reflections
Intensity decay (%)	1	1	1
Refinement			
Refinement on	F	F	F
R	0.0424	0.0498	0.0473
wR	0.0399	0.0442	0.0392
S	1.1155	1.1732	0.9200
Occupation ratio			
α [site (1)]	0.384 (3)	0.393 (4)	0.387 (3)
β [site (2)]	0.159 (2)	0.173 (3)	0.187 (2)
x [$x = (\alpha + \beta)/2$]	0.271	0.283	0.287
No. of reflections used in refinement	2000	1989	1937
No. of parameters used	197	197	197
H-atom treatment	H atoms: see text	H atoms: see text	H atoms: see text
Weighting scheme	$w = 1/[\sigma(F_o)^2 + (0.015F_o)^2]$	$w = 1/[\sigma(F_o)^2 + (0.015F_o)^2]$	$w = 1/[\sigma(F_o)^2 + (0.015F_o)^2]$
$(\Delta/\sigma)_{max}$	<0.025	<0.021	<0.032
$\Delta\rho_{max}$ (e Å^{-3})	0.56	0.57	0.54
$\Delta\rho_{min}$ (e Å^{-3})	−0.51	−0.47	−0.58
Extinction method	Zachariasen (1967)	Zachariasen (1967)	Zachariasen (1967)
Extinction coefficient	$g = 2.0443 \times 10^{-4}$	$g = 3.973 \times 10^{-4}$	$g = 1.484 \times 10^{-4}$
Source of atomic scattering factors	*International Tables for X-ray Crystallography* (1974, Vol. IV) and Stewart, Davidson & Simpson (1965)	*International Tables for X-ray Crystallography* (1974, Vol. IV) and Stewart, Davidson & Simpson (1965)	*International Tables for X-ray Crystallography* (1974, Vol. IV) and Stewart, Davidson & Simpson (1965)

reported by Suzuki, Muta, Nozaki & Shiozaki (1996) were used and also these parameters were fixed during the refinements. The results of α, β and the values of x at each temperature are given in Table 1. The value of x shows a good correspondence with the result of the dielectric measurement within experimental error. The final results of the atomic positions and equivalent thermal parameters at the three temperatures are given in Table 2.*

* Lists of anisotropic displacement parameters, H-atom coordinates and structure factors have been deposited with the IUCr (Reference: OH0056). Copies may be obtained through The Managing Editor, International Union of Crystallography, 5 Abbey Square, Chester CH1 2HU, England.

Table 2. *Fractional atomic coordinates and equivalent isotropic displacement parameters ($\times 10^4$ Å^2) for non-H atoms at $T = 213$ (first row), 253 (second row) and 293 K (third row)*

$U_{eq} = 1/3\Sigma U_{ij} a_i^* a_j^* \mathbf{a}_i.\mathbf{a}_j$

	x	y	z	U_{eq}	Occupancy†
Na	0.26861 (7)	0.49267 (6)	0.47909 (12)	194 (4)	
	0.26889 (8)	0.49286 (7)	0.47729 (15)	228 (5)	
	0.26904 (8)	0.49290 (7)	0.47620 (12)	266 (5)	
KN(1)	0.0	0.0	0.0449 (2)	425 (8)	0.384 (3)
	0.0	0.0	0.0462 (3)	507 (11)	0.393 (4)
	0.0	0.0	0.0474 (3)	588 (12)	0.387 (3)
KN(2)	0.0	0.5	0.1620 (1)	218 (4)	0.159 (2)
	0.0	0.5	0.1608 (2)	255 (5)	0.173 (3)
	0.0	0.5	0.1599 (2)	289 (5)	0.187 (2)
C(1)	0.1550 (2)	0.1883 (1)	0.2835 (3)	145 (9)	
	0.1544 (2)	0.1881 (2)	0.2849 (4)	167 (11)	
	0.1543 (2)	0.1882 (2)	0.2846 (4)	185 (11)	
C(2)	0.1254 (2)	0.2737 (1)	0.4230 (3)	145 (9)	
	0.1255 (2)	0.2735 (2)	0.4235 (4)	163 (11)	
	0.1255 (2)	0.2736 (2)	0.4240 (4)	176 (10)	
C(3)	0.1787 (2)	0.2638 (1)	0.6459 (3)	143 (8)	
	0.1788 (2)	0.2639 (2)	0.6453 (4)	171 (10)	
	0.1789 (2)	0.2641 (2)	0.6452 (4)	194 (11)	
C(4)	0.1529 (2)	0.3516 (2)	0.7811 (3)	184 (10)	
	0.1536 (3)	0.3517 (2)	0.7805 (4)	215 (12)	
	0.1540 (3)	0.3524 (2)	0.7787 (4)	242 (12)	
O(1)	0.1203 (1)	0.1088 (1)	0.3508 (3)	181 (7)	
	0.1203 (2)	0.1091 (1)	0.3521 (3)	216 (9)	
	0.1201 (2)	0.1093 (1)	0.3527 (3)	253 (9)	
O(2)	0.2095 (1)	0.2032 (1)	0.1171 (2)	218 (8)	
	0.2087 (2)	0.2027 (1)	0.1178 (3)	256 (9)	
	0.2085 (2)	0.2025 (1)	0.1183 (3)	303 (10)	
O(3)	0.2333 (2)	0.4060 (1)	0.8149 (2)	267 (8)	
	0.2341 (2)	0.4059 (1)	0.8134 (3)	308 (10)	
	0.2346 (2)	0.4059 (1)	0.8119 (3)	347 (10)	
O(4)	0.0538 (2)	0.3620 (1)	0.8445 (3)	270 (8)	
	0.0546 (2)	0.3626 (1)	0.8435 (3)	308 (10)	
	0.0554 (2)	0.3630 (1)	0.8424 (3)	355 (10)	
O(5)	0.1650 (1)	0.3575 (1)	0.3246 (3)	193 (7)	
	0.1645 (2)	0.3571 (1)	0.3242 (3)	221 (9)	
	0.1641 (2)	0.3570 (1)	0.3240 (3)	258 (9)	
O(6)	0.2963 (2)	0.2478 (1)	0.6291 (3)	218 (8)	
	0.2958 (2)	0.2478 (2)	0.6278 (4)	249 (10)	
	0.2954 (2)	0.2479 (1)	0.6272 (3)	281 (10)	
O(7)	0.3951 (2)	0.0825 (2)	0.4797 (4)	245 (9)	
	0.3949 (2)	0.0824 (2)	0.4800 (4)	289 (12)	
	0.3952 (2)	0.0827 (2)	0.4814 (4)	337 (12)	
O(8)	0.2466 (2)	0.0410 (1)	0.8825 (3)	410 (11)	
	0.2476 (3)	0.0414 (2)	0.8844 (3)	444 (13)	
	0.2482 (3)	0.0414 (2)	0.8855 (3)	511 (14)	
O(9)	0.4375 (2)	0.3003 (2)	0.0383 (4)	448 (13)	
	0.4365 (3)	0.2989 (3)	0.0397 (5)	523 (18)	
	0.4357 (3)	0.2976 (3)	0.0397 (5)	600 (19)	
O(10)	0.4238 (2)	0.3957 (2)	0.4222 (5)	481 (14)	
	0.4250 (2)	0.3977 (2)	0.4181 (5)	562 (18)	
	0.4253 (2)	0.3986 (2)	0.4149 (5)	637 (18)	

† No entry indicates occupancy 1.0.

3. Discussion

3.1. *Displacements of atoms with temperature change*

An *ORTEP*II plot (Johnson, 1976) of one-quarter of the unit cell at $T = 213$ K is given in Fig. 1. As temperature decreases, the positions of several atoms are varied. The positions of KN(1) and KN(2) are shifted in the opposite direction along the c axis. In the tartrate molecules the carboxylate anion O(3)—C(4)—O(4) is displaced along the a axis. O(8), bonded to O(3) and O(2) by hydrogen bonds, is displaced in the direction opposite to the shift of the carboxylate anion. The collected displacements of the carboxylate anion and oxygen are the same as those observed in the ferroelectric phase transition of RS (Suzuki & Shiozaki, 1996). O(9) and O(10) show large shifts as the temperature decreases: O(9) is shifted in the direction of KN(1), on the other hand, O(10) is shifted in the opposite direction. Those atoms have large atomic and molecular displacements with temperature changes in the paraelectric phase and this fact suggests that the mechanism of the phase transition is not of simple order–disorder character. It should be clarified how these displacements in the paraelectric phase are related to the crystal structure in the ferroelectric phase.

3.2. *Temperature dependence of interatomic distances*

The bond distances and angles in the tartrate molecules (Table 3) are kept almost constant and the interatomic distances between sodium and oxygens (Table 4) show small changes.

The changes in the interatomic distances between KN(1) and oxygens are remarkable (Table 5). The KN(1)—O(1) distance is almost kept constant, while those of KN(1)—O(8) and KN(1)—O(9) are shortened as temperature decreases and that of KN(1)—O(10) is lengthened. On the other hand, the changes in the distances between KN(2) and oxygens are small.

In this crystal ($x = 0.28$) KN(2)—O(8) is smaller than KN(1)—O(8). On the other hand, in RS (Suzuki & Shiozaki, 1996) the K(2)—O(8) distance

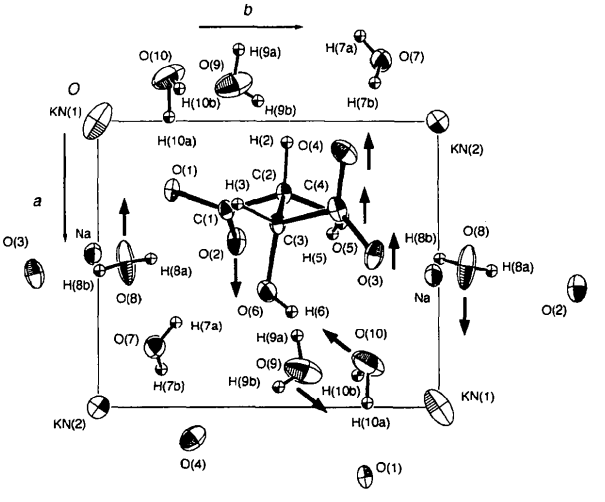

Fig. 1. Projection of the asymmetric unit of the crystal structure of the paraelectric phase of $NaK_{0.72}(NH_4)_{0.28}(+)$-$C_4H_4O_6.4H_2O$ ($T = 213$ K) on (001). Thermal ellipsoids are drawn at the 50% probability level using *ORTEP*II (Johnson, 1976). H atoms are drawn as small spheres. Arrows indicate the directions of the atomic shifts as the temperature lowers.

Table 3. *Bond lengths (Å) and angles (°) of the tartrate molecules in $RS_{0.72}ARS_{0.28}$*

	213 K	253 K	293 K
C(1)—C(2)	1.536 (3)	1.535 (3)	1.538 (3)
C(2)—C(3)	1.529 (3)	1.526 (3)	1.525 (3)
C(3)—C(4)	1.539 (3)	1.541 (3)	1.542 (3)
C(1)—O(1)	1.278 (2)	1.270 (3)	1.274 (3)
C(1)—O(2)	1.239 (2)	1.242 (3)	1.239 (3)
C(2)—O(5)	1.423 (2)	1.424 (3)	1.424 (3)
C(2)—H(2)	1.07 (2)	1.06 (3)	1.07 (2)
C(3)—O(6)	1.421 (3)	1.419 (3)	1.417 (3)
C(3)—H(3)	1.08 (2)	1.03 (3)	1.05 (2)
C(4)—O(3)	1.250 (3)	1.251 (3)	1.249 (3)
C(4)—O(4)	1.252 (3)	1.254 (4)	1.253 (4)
O(2)—O(5)	2.605 (2)	2.607 (2)	2.610 (2)
O(5)—H(5)	0.78 (3)	0.80 (4)	0.78 (3)
H(5)···O(2)	2.11 (3)	2.06 (3)	2.12 (3)
O(3)—O(6)	2.645 (2)	2.643 (3)	2.641 (3)
O(6)—H(6)	0.69 (4)	0.65 (4)	0.65 (4)
H(6)···O(3)	2.46 (4)	2.38 (5)	2.36 (4)
O(1)—C(1)—O(2)	126.5 (2)	126.3 (2)	126.4 (2)
O(1)—C(1)—C(2)	116.5 (2)	116.8 (2)	116.4 (2)
O(2)—C(1)—C(2)	117.0 (2)	116.9 (2)	117.2 (2)
C(1)—C(2)—O(5)	110.4 (2)	110.5 (2)	110.3 (2)
C(1)—C(2)—C(3)	110.0 (2)	110.0 (2)	110.2 (2)
O(5)—C(2)—C(3)	109.2 (2)	109.4 (2)	109.6 (2)
C(2)—O(5)—H(5)	108 (2)	105 (2)	109 (2)
C(2)—C(3)—O(6)	110.9 (2)	110.8 (2)	110.8 (2)
C(2)—C(3)—C(4)	109.6 (2)	109.8 (2)	109.5 (2)
O(6)—C(3)—C(4)	111.6 (2)	111.5 (2)	111.5 (2)
C(3)—O(6)—H(6)	121 (3)	116 (4)	115 (4)
C(3)—C(4)—O(4)	117.1 (2)	117.1 (2)	116.8 (2)
C(3)—C(4)—O(3)	116.4 (2)	116.3 (2)	116.3 (2)
O(3)—C(4)—O(4)	126.5 (2)	126.6 (2)	126.8 (2)
O(5)—H(5)···O(2)	121 (5)	125 (3)	121 (3)
O(6)—H(6)···O(3)	98 (4)	107 (4)	109 (4)

Table 4. *Interatomic distances (Å) around Na atoms*

	213 K	253 K	293 K
Na—O(1^{i})	2.369 (2)	2.374 (2)	2.382 (2)
Na—O(3)	2.461 (2)	2.468 (2)	2.469 (2)
Na—O(5)	2.483 (2)	2.494 (2)	2.502 (2)
Na—O(7^{i})	2.346 (2)	2.351 (3)	2.362 (3)
Na—O(8^{i})	2.356 (2)	2.363 (2)	2.367 (2)
Na—O(10)	2.335 (3)	2.335 (3)	2.336 (3)
Mean	2.392	2.398	2.403

Symmetry code: (i) $\frac{1}{2}-x, \frac{1}{2}+y, 1-z$.

is larger than K(1)—O(8). In the $RS_{1-x}ARS_x$ mixed crystal [$0.90 < x < 1.00$ (Suzuki, Muta, Nozaki & Shiozaki, 1996)], N(2)—O(8) is also larger than N(1)—O(8). Our results show that the position of O(8) in region III is closer to site (1) than those in regions (I) and (IV).

The distances between the oxygens, which are bonded through the hydrogen bonds, are kept almost constant, except O(6)—O(10) (Table 6). The O(6)—O(10) distance is greatly shortened as temperature decreases. As mentioned above, the atomic positions of O(9) and O(10) are greatly shifted, however, the O(9)—O(10) distance is kept constant, which indicates that O(9) and O(10) are displaced collectively.

Table 5. *Interatomic distances (Å) around KN(1) and KN(2)*

	213 K	253 K	293 K
KN(1)—O(1)	2.841 (2)	2.849 (2)	2.851 (2)
KN(1^{i})—O(9)	2.990 (3)	3.021 (4)	3.047 (4)
KN(1)—O(8^{ii})	3.157 (3)	3.176 (3)	3.190 (3)
KN(1)—O(10^{iii})	3.384 (3)	3.359 (3)	3.347 (3)
KN(2)—O(4^{ii})	2.860 (2)	2.860 (2)	2.864 (2)
KN(2^{iv})—O(7)	2.810 (2)	2.820 (3)	2.823 (3)
KN(2)—O(5)	3.003 (2)	3.010 (2)	3.015 (2)
KN(2)—O(8^{v})	3.085 (3)	3.081 (3)	3.081 (3)

Symmetry codes: (i) $\frac{1}{2}+x, \frac{1}{2}-y, -z$; (ii) $x, y, z-1$; (iii) $x-\frac{1}{2}, \frac{1}{2}-y, -z$; (iv) $\frac{1}{2}+x, \frac{1}{2}-y, 1-z$; (v) $\frac{1}{2}-x, \frac{1}{2}+y, 1-z$.

Table 6. *Hydrogen-bond geometry (Å, °)*

	O—H	O···O	O···H	O—H···O
T = 213 K				
O(6)—H(6)···O(10)	0.69 (4)	2.901 (3)	2.24 (4)	160 (4)
O(7)—H(7a)···O(6)	0.64 (5)	2.794 (3)	2.18 (5)	162 (7)
O(7)—H(7b)···O(4^{i})	0.96 (3)	2.872 (3)	1.97 (3)	156 (3)
O(8)—H(8a)···O(3^{ii})	0.86 (3)	2.703 (2)	1.85 (3)	169 (3)
O(8)—H(8b)···O(2^{iii})	0.72 (3)	2.771 (2)	2.06 (3)	167 (4)
O(9)—H(9a)···O(2)	0.78 (4)	3.085 (3)	2.45 (4)	139 (3)
O(9)—H(9b)···O(4^{i})	0.67 (4)	2.796 (3)	2.15 (4)	166 (4)
O(10)—H(10a)···O(9)	0.81 (4)	2.751 (4)	2.01 (4)	152 (4)
O(10)—H(10b)···O(1^{i})	0.89 (4)	2.731 (3)	1.86 (3)	166 (3)
	Angle			
H(7a)—O(7)—H(7b)	118 (6)			
H(8a)—O(8)—H(8b)	91 (3)			
H(9a)—O(9)—H(9b)	117 (5)			
H(10a)—O(10)—H(10b)	92 (4)			
	O—H	O···O	O···H	O—H···O
T = 253 K				
O(6)—H(6)···O(10)	0.65 (4)	2.944 (4)	2.36 (5)	152 (5)
O(7)—H(7a)···O(6)	0.61 (4)	2.799 (3)	2.19 (4)	177 (5)
O(7)—H(7b)···O(4^{i})	0.96 (4)	2.881 (3)	1.98 (4)	156 (4)
O(8)—H(8a)···O(3^{ii})	0.82 (3)	2.708 (3)	1.90 (4)	170 (4)
O(8)—H(8b)···O(2^{iii})	0.86 (4)	2.765 (3)	1.91 (4)	173 (4)
O(9)—H(9a)···O(2)	0.77 (5)	3.084 (4)	2.43 (5)	144 (4)
O(9)—H(9b)···O(4^{i})	0.74 (5)	2.800 (4)	2.06 (5)	174 (5)
O(10)—H(10a)···O(9)	0.81 (4)	2.750 (4)	1.97 (5)	160 (4)
O(10)—H(10b)···O(1^{i})	0.87 (4)	2.736 (4)	1.88 (4)	169 (3)
	Angle			
H(7a)—O(7)—H(7b)	110 (5)			
H(8a)—O(8)—H(8b)	102 (3)			
H(9a)—O(9)—H(9b)	102 (5)			
H(10a)—O(10)—H(10b)	95 (4)			
	O—H	O···O	O···H	O—H···O
T = 293 K				
O(6)—H(6)···O(10)	0.65 (4)	2.969 (4)	2.40 (4)	149 (5)
O(7)—H(7a)···O(6)	0.66 (5)	2.800 (3)	2.16 (5)	163 (5)
O(7)—H(7b)···O(4^{i})	0.88 (4)	2.888 (3)	2.06 (4)	157 (4)
O(8)—H(8a)···O(3^{ii})	0.74 (3)	2.712 (2)	1.98 (3)	170 (3)
O(8)—H(8b)···O(2^{iii})	0.87 (4)	2.767 (3)	1.90 (4)	176 (4)
O(9)—H(9a)···O(2)	0.82 (4)	3.077 (4)	2.40 (4)	141 (4)
O(9)—H(9b)···O(4^{i})	0.66 (5)	2.806 (4)	2.15 (5)	170 (5)
O(10)—H(10a)···O(9)	0.86 (4)	2.752 (5)	1.92 (4)	161 (4)
O(10)—H(10b)···O(1^{i})	0.84 (4)	2.745 (3)	1.91 (3)	172 (3)
	Angle			
H(7a)—O(7)—H(7b)	112 (5)			
H(8a)—O(8)—H(8b)	100 (4)			
H(9a)—O(9)—H(9b)	117 (5)			
H(10a)—O(10)—H(10b)	96 (3)			

Symmetry codes: (i) $\frac{1}{2}+x, \frac{1}{2}-y, 1-z$; (ii) $\frac{1}{2}-x, y-\frac{1}{2}, 2-z$; (iii) $x, y, 1+z$.

3.3. *Temperature dependence of thermal motions of oxygens in the water molecules*

The amplitudes of the atomic thermal motions in the crystal are obtained as thermal parameters U_{ij} in the crystal structure analysis. The temperature dependence of the equivalent thermal parameters (U_{eq}) of each oxygen in the four water molecules is given in Fig. 2. Among them, the temperature dependence of the thermal parameters of O(8) is different from the rest. The slope line related with O(8) is linear and approaches a positive value at zero temperature.

Itoh (1984) has discussed the temperature dependence of the mean-square thermal displacement of the disordered atom in ferroelectrics. The extrapolated line obtained in the paraelectric phase does not pass through the origin and has a positive value at $T = 0$ K. In such a way, Itoh has presented a method of showing the disordered atom. According to Itoh's criterion, O(8) is the disordered atom in the paraelectric phase; however, no sign of the disordered state of O(8) is observed in the difference-Fourier syntheses.

From the above-mentioned results, we can conclude the following: Firstly, it is clarified that in the paraelectric phase the atomic positions of O(8), O(9) and O(10) and the carboxylate anion O(3)—C(4)—O(4) are displaced with temperature changes. Secondly, the anomalous temperature dependence of the thermal parameter of O(8) is observed. One of the possible interpretations is the disordered state of O(8). The thermal motion of O(8), especially along the a axis, behaves anomalously and the fact suggests that O(8) has an important role for the phase transition of $RS_{1-x}ARS_x$.

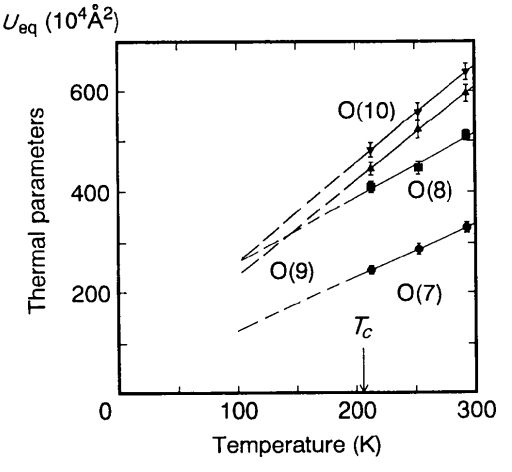

Fig. 2. Temperature dependence of the thermal parameters of the four oxygens [O(7), O(8), O(9) and O(10)] in the water molecules. U_{eq} represents the equivalent thermal parameters.

Now an X-ray study of this mixed crystal in the ferroelectric phase is in progress. Together with the study of the ferroelectric phase, the mechanism of the phase transition of $RS_{1-x}ARS_x$ in region III will be clarified.

The authors wish to express their thanks to Mr H. Toki for the preparation of the sample and to Mr K. Ańdo for the dielectric measurements.

References

Beevers, C. A. & Hughes, W. (1941). *Proc. R. Soc. A*, **177**, 251–259.
Brózek, Z. & Stadnicka, K. (1994). *Acta Cryst.* B**50**, 59–68.
Brózek, Z., Mucha, D. & Stadnicka, K. (1994). *Acta Cryst.* B**50**, 465–472.
Coppens, P., Guru Row, T. N., Leung, P., Stevens, E. D., Becker, P. J. & Yang, Y. W. (1979). *Acta Cryst.* A**35**, 63–72.
Dwiggins, C. W. Jr (1975). *Acta Cryst.* A**31**, 395–396.
El Saffar, Z. M. & Pope, G. (1976). *J. Phys. Soc. Jpn*, **48**, 2003–2006.
Gesi, K. & Ozawa, K. (1980). *J. Chem. Phys.* **64**, 2696.
Itoh, K. (1984). *J. Phys. Soc. Jpn*, **53**, 2049–2053.
Johnson, C. K. (1976). *ORTEP*II. Report ORNL-5138. Oak Ridge National Laboratory, Tennessee, USA.
Jona, F. & Shirane, G. (1962). *Ferroelectric Crystals*, pp. 280–317. Oxford: Pergamon Press.
Makita, Y. & Takagi. Y. (1958). *J. Phys. Soc. Jpn*, **13**, 367–377.
Stewart, R. E., Davidson, E. R. & Simpson, W. T. (1965). *J. Chem. Phys.* **42**, 3175–3187.
Suzuki, E. & Shiozaki, Y. (1996). *Phys. Rev. B*, **53**, 5217–5221.
Suzuki, E., Muta, T., Nozaki, R. & Shiozaki, Y. (1996). *Acta Cryst.* B**52**, 296–302.
Takagi, Y. & Makita, Y. (1958). *J. Phys. Soc. Jpn*, **13**, 272–277.
Zachariasen, W. H. (1967). *Acta Cryst.* **23**, 558–564.